AIAA 81-4292

Implicit Noniterative Schemes for Unsteady Boundary Layers

P. Orlandi* and J.H. Ferziger†
Stanford University, Stanford, Calif.

In order to solve unsteady boundary layers it is necessary to use fast and stable methods; implicit methods are therefore very useful. To overcome the iterative procedure related to the nonlinear system of equations, a linearization procedure should be employed. In this paper the method developed by Beam and Warming has been applied for both time and streamwise directions. Due to the time-dependent coordinate transformation and to the nonlinearity, the Beam-Warming algorithm does not retain a large number of time-differencing schemes. The method has been applied to unsteady laminar boundary layers and the solutions compared with the analytical and experimental results.

Nomenclature

a = stretching parameter
A = $(d\xi/dx_1)^{-1}$ = function of transformation
AC, AM, AP = coefficients of the block tridiagonal system
B = $(d\eta/dx_2)^{-1}/S$ = function of transformation
C = $-\eta(\partial S/\partial t)(d\eta/dx_2)^{-1}/S$ = function of transformation
C_f = skin friction
D = $-\eta(\partial S/\partial x)(d\eta/dx_2)^{-1}/S$ = function of transformation
E = $(d\eta/dx_2)^{-1}$ = function of transformation
f = dimensionless stream function
F = $(d\eta/dx_2)^{-1}/ReS^2$ = function of transformation
g = first derivative of f with respect to η
G = $(d\eta/dx_2)^{-1}(d\xi/dx_1)^{-1}/S$ = function of transformation
H = $-(\partial S/\partial x)(d\eta/dx_2)^{-1}/S^2$ = function of transformation
L = $(d\eta/dx_2)^{-1}/S^2$ = function of transformation
m = $x(\partial U_e/\partial x)/U_e$ = pressure gradient parameter
Re = Reynolds number
S = function of x and t to scale vertical direction
t = dimensionless time
U = dimensionless horizontal velocity
U_e = dimensionless edge velocity
U_1 = dimensionless amplitude of the oscillating part of U_e
V = dimensionless vertical velocity
x = dimensionless downstream coordinate
x_0 = initial value of the downstream coordinate
x_1, x_2 = coordinates of uniform spacing
x_s = points of zero skin friction
y = dimensionless vertical coordinate
α = amplitude of the Howarth edge velocity
γ = phase angle of the horizontal velocity
δ = dimensionless boundary-layer thickness
δU_1 = dimensionless amplitude of the oscillating part of U_1
$\Delta x_1, \Delta x_2$ = mesh size
Δt = time step
$\Delta(\ )$ = forward operator
$\nabla(\ )$ = backward operator
η = scaled vertical coordinate
η_∞ = η evaluated at the edge of the computation
θ, ζ = parameters of the implicit scheme
ω = dimensionless frequency

Received Oct. 24, 1980; revision received April 7, 1981.

*Associate Professor, Institute of Aerodynamics, University of Rome, Italy; Visiting Professor, Stanford University, 1978.
†Professor, Mechanical Engineering Department. Member AIAA.

I. Introduction

NUMERICAL solution of unsteady laminar boundary-layer equations has been the subject of considerable study in the recent years. There is still much to do, especially for turbulent flows where the numerical results differ widely and depend on both the numerics and the turbulence modeling. All investigators use implicit methods to remove the stability limitations on the time step and the grid size in the downstream direction.[1] To solve the unsteady boundary-layer equations the most common method consists of two principal parts: 1) the coordinate normal to the flow is transformed in a manner well suited to the laminar case; and 2) the resulting equations are written as a system of first-order partial differential equations and solved with a Newton-Raphson scheme such as the Keller box algorithm (KBS).[2] This procedure requires many iterations for complex flowfields.

We chose to use the transformation introduced by Nash,[3] that is, we shall transform the normal coordinate by normalizing on the boundary-layer thickness as a function of both downstream distance and time. In the laminar case there is not a great difference; the advantage of this transformation is mainly in treating turbulent flows. The singularity at a stagnation point cannot be treated with this transformation. In the KBS the equations are discretized by the finite-volume approach; we shall use finite differences. The continuity equation will be differentiated with respect to the coordinate normal to the wall; thus we are dealing with a system of second-order partial differential equations.

To solve the nonlinear system of equations a noniterative, implicit, finite-difference algorithm has been used. It consists of linearizing the system of equations with the same accuracy employed to discretize the derivatives. This linearization scheme has been developed by Briley and McDonald[4] for the compressible Navier-Stokes equations and by Beam and Warming, who have used the scheme for both inviscid and viscous gasdynamic equations.[5,6] The system of equations considered by Beam and Warming is parabolic in time and their coordinate transformation does not depend on time; thus their algorithm was written in "delta" form and can be put in a general form which includes a large number of time-differencing methods. Since the boundary-layer equations are parabolic both in time and the streamwise coordinate, two approaches can be considered. If the primary marching is in the x direction, the system of equations must be linearized with respect to time; due to the time-dependent normal coordinate transformation, the general formulation does not retain the large number of time-differencing options as those of Beam and Warming.

In the computation of unsteady boundary layers, especially with adverse pressure gradients, it is worthwhile to treat time as the primary marching direction. In this case the noniterative algorithm is applied to the downstream differencing. Due to the nonlinearity, the approximation cannot

be written in a generalized form that contains a variety of schemes. Moreover, it must be used also in differencing the continuity equation in the downstream direction. This marching procedure has a more general validity. In fact, if the time dependence is neglected, the steady boundary-layer equations are recovered.

To discretize the equations in the vertical direction, coordinate stretching using an analytical coordinate transformation has been chosen; the derivatives of the transformation are computed by finite differences. In this way, the truncation errors are reduced with respect to the case in which the derivatives are analytically computed.[7] In the laminar case, an optimum value of the stretching parameter has been found, as suggested by Blottner.[8] Coordinate stretching has also been used in the downstream direction. This is useful for dealing with flows containing a small recirculating region but for which the boundary-layer approximation is valid. In such cases more computational points are needed near the separation and reattachment points.

This method of solving steady and unsteady boundary layers has been tested in cases for which analytical and experimental solutions are available in the literature. Moreover, a case of a strong adverse pressure gradient with superimposed unsteadiness has been considered. The effect is to delay the separation farther downstream as the frequency is increased. In all cases the computation is taken to the separation point.

II. Boundary-Layer Transformation

The nondimensional continuity and momentum equations for the unsteady, incompressible laminar boundary layer are:

Continuity equation

$$\frac{\partial U}{\partial x}+\frac{\partial V}{\partial y}=0 \tag{1}$$

Momentum equation

$$\frac{\partial U}{\partial t}+U\frac{\partial U}{\partial x}+V\frac{\partial U}{\partial y}=\frac{\partial U_e}{\partial t}+U_e\frac{\partial U_e}{\partial x}+\frac{1}{Re}\frac{\partial^2 U}{\partial y^2} \tag{2}$$

To solve the system of Eqs. (1) and (2), it is useful to normalize the normal coordinate with respect to the boundary-layer thickness. We have chosen to transform Eqs. (1) and (2) with respect to a function $S(x,t)$ which is allowed to increase or decrease according to the boundary-layer thickness.[3] Thus the independent variables have been transformed as

$$t=t, \qquad x=\xi(x_1), \qquad y=S(x_1,t)\eta(x_2) \tag{3}$$

where x_1 and x_2 are the new coordinates and $\xi(x_1)$ and $\eta(x_2)$ are stretching functions introduced to give more computational points in regions where larger gradients of the physical quantities occur. Introducing Eq. (3) in the momentum equation (2) we have

$$\frac{\partial U}{\partial t}+AU\frac{\partial U}{\partial x_1}+BV\frac{\partial U}{\partial x_2}+C\frac{\partial U}{\partial x_2}+DU\frac{\partial U}{\partial x_2}$$

$$=\frac{\partial U_e}{\partial t}+U_e\frac{\partial U_e}{\partial x}+F\frac{\partial}{\partial x_2}\left(E\frac{\partial U}{\partial x_2}\right) \tag{4}$$

where A, B, C, D, E, and F are functions of the transformation and of the derivatives with respect to the new coordinate system.

Instead of using the continuity equation (1), we differentiated it with respect to the y coordinate. The reason is that we wish to discretize the momentum and the continuity equations in the grid points (I,J). If Eq. (1) is used, the matrix associated to the vertical velocity does not have a diagonal dominance, and it is difficult to evaluate the coefficients of the matrix at the upper boundary. The conventional approach[1] to discretize Eq. (1) in the midpoints $(J-\frac{1}{2})$ requires interpolations for the horizontal velocity and the new coordinate $\eta(x_2)$. Differentiating Eq. (1) with respect to y, the matrix associated with the vertical velocity has a diagonal dominance. Another boundary condition, where the freestream velocity gradient appears, is required. The approach described in this paper and the conventional one[1] present both advantages and disadvantages, so it is difficult to say which one is better.

Introducing the coordinate transformation [Eq. (3)] into the differentiated continuity equation, we have

$$G\frac{\partial^2 U}{\partial x_1\partial x_2}+H\eta\frac{\partial}{\partial x_2}\left(E\frac{\partial U}{\partial x_2}\right)+L\frac{\partial}{\partial x_2}\left(E\frac{\partial V}{\partial x_2}\right)=0 \tag{5}$$

The boundary conditions at the wall and the outer edge of the boundary layer are

$$\begin{aligned} &y=0, && U=V=0\\ &y\to\infty, && U=U_e, \qquad \partial V/\partial y=-\partial U_e/\partial x \end{aligned} \tag{6}$$

To complete the formulation of the problem, initial conditions must be assigned. In all the cases a Blasius profile has been imposed at $t=0$ for $x\geq x_0$ and at $x=x_0$ for $t\geq 0$. The Blasius profile was generated by solving the third-order equation obtained by introducing the Falkner-Skan transformation[9] into Eqs. (1) and (2) and assuming the flow to be self-similar

$$f'''+(m+1)/2ff''+m(1-f'^2)=0 \tag{7}$$

where the prime means derivative with respect to the similarity variable $\eta=(Re/x)^{1/2}y$. For the same reason as the differentiation of the continuity equations, we reduced Eq. (7) to a system of two second-order differential equations

$$g''+(m+1)/2fg'+m(1-g^2)=0 \tag{8a}$$

$$f''-g'=0 \tag{8b}$$

with the boundary conditions

$$\eta=0, \quad f=g=0; \quad \eta=\infty, \quad f'=g=1 \tag{9}$$

The solution of Eq. (8) was a test case to prove the validity of introducing higher-order derivatives and for testing the coordinate stretching in the vertical direction.

III. Numerical Scheme

A. Finite-Difference Scheme in the Normal Direction

To solve the nonlinear system of Eqs. (8), Newton's method has been used. The unknowns at the $(n+1)$st iteration are expressed in the form

$$(f^{n+1},g^{n+1})=(f^n,g^n)+(\Delta f^n,\Delta g^n) \tag{10}$$

Using Eq. (10) in Eq. (8) and dropping the quadratic terms, a linear system of differential equations is obtained. If coordinate stretching $\eta(x_2)$ and a uniform grid Δx_2 is used, the first and second derivatives are

$$\frac{df}{d\eta}=\frac{df}{dx_2}\frac{dx_2}{d\eta}=\frac{f_{J+1}-f_{J-1}}{2\Delta x_2}\left(\frac{d\eta}{dx_2}\right)_J^{-1}+O(\Delta x_2^2) \tag{11}$$

$$\frac{d^2f}{d\eta^2}=\frac{d}{dx_2}\left[\left(\frac{d\eta}{dx_2}\right)^{-1}\frac{df}{dx_2}\right]\left(\frac{d\eta}{dx_2}\right)^{-1}$$

$$= \left[\frac{f_{J+1}-f_J}{\Delta x_2}\left(\frac{d\eta}{dx_2}\right)^{-1}_{J+\frac{1}{2}} - \frac{f_J-f_{J-1}}{\Delta x_2}\left(\frac{d\eta}{dx_2}\right)^{-1}_{J-\frac{1}{2}}\right]$$

$$\times \left(\frac{d\eta}{dx_2}\right)^{-1}_J + O(\Delta x_2^2) \tag{12}$$

The particular coordinate transformation used is

$$\eta = (\tanh ax_2/\tanh a)\,\eta_\infty \tag{13}$$

where a is a parameter; larger a gives more mesh points near the wall. The derivatives of the coordinate transformation have been computed by a centered finite-difference scheme. The discretization of the linear system of equations yields a block tridiagonal system of linear equations

$$AP_{k,i,J}(\Delta q_i^n)_{J+1} + AC_{k,i,J}(\Delta q_i^n)_J + AM_{k,i,J}(\Delta q_i^n)_{J-1} = DC_J \tag{14}$$

where the index i in Δq_i^n refers to the unknown quantities ($\Delta q_1^n = \Delta g^n$ and $\Delta q_2^n = \Delta f^n$). The indices k and i in the coefficients AP, AC, and AM are related, respectively, to the number of equations [$k=1$, Eq. (8a); $k=2$, Eq. (8b)] and to the unknown quantities. The system of equations (14) is solved by an efficient elimination procedure. As shown by Blottner,[8] the laminar case requires less stretching than the turbulent case.

The error in the skin friction vs the stretching parameter a is plotted in Fig. 1 for two different mesh sizes. A comparison of the results obtained with this procedure and the KBS and variable grid scheme (VGS) of Blottner[8] is shown in Fig. 2, in which the error in the skin friction is plotted vs the number of calculational points. As expected, the optimum stretching parameter decreases as the number of points is increased.

B. Linearization for Time Advancement

Following the procedure of Beam and Warming,[6] the temporal discretization can be expressed in a Padé form:

$$\frac{\partial U^n}{\partial t} = \frac{1}{\Delta t}\left[\frac{(1+\zeta)\Delta - \zeta\nabla}{1+\theta\Delta}\right]U^n + (\theta-\zeta-\tfrac{1}{2})O(\Delta t) + O(\Delta t^2) \tag{15}$$

where Δ is the forward difference operator $\Delta U^n \equiv (U^{n+1} - U^n)$ and ∇ is the backward difference operator $\nabla U^n \equiv (U^n - U^{n-1})$. Adjusting the constants ζ and θ Eq. (15) gives a number of time-differencing approximations, implicit and explicit, first- and second-order accurate. Applying Eq. (15) to the momentum equation (4), written as $(\partial U/\partial t) = M_t$, we have

$$(\theta\Delta M_t^n + M_t^n)\Delta t/(1+\zeta)$$

$$= \Delta U^n - [\zeta/(1+\zeta)]\nabla U^n + O[(\theta-\zeta-\tfrac{1}{2})\Delta t^2 + \Delta t^3] \tag{16}$$

Applying the Δ operator to each term of this equation yields a linear partial differential equation for ΔU^n and ΔV^n. To illustrate this, consider the application of this operator to $Ap(\partial U/\partial x_k)$, where p can be U or V, and A may be a function of both time and space.

When the operator on the left-hand side of Eq. (16) is applied to $Ap(\partial U/\partial x_k)$, we obtain

$$\left\{A^{n+1}\left[\theta\left(\Delta p^n\left(\frac{\partial U}{\partial x_k}\right)^n + p^n\frac{\partial \Delta U^n}{\partial x_k}\right) + \left(p\frac{\partial U}{\partial x_k}\right)^n\right]\right.$$

$$\left. + (\theta-1)\Delta A^n\left(p\frac{\partial U}{\partial x_k}\right)^n\right\}\frac{\Delta t}{1+\zeta} + O(\Delta p \Delta U \Delta t) \tag{17}$$

The accuracy of the equation resulting from setting this equal to the right-hand side of Eq. (16) is of the same order as the truncation error of Eq. (16), because Δp and ΔU are

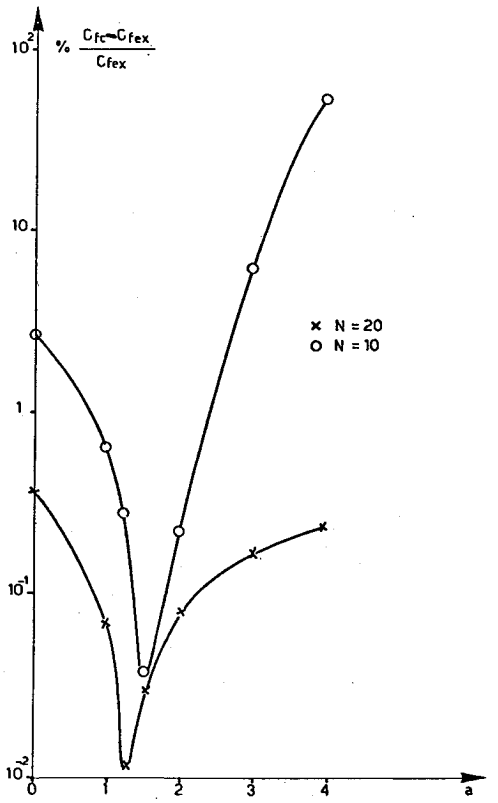

Fig. 1 Accuracy of the skin friction, with different grids.

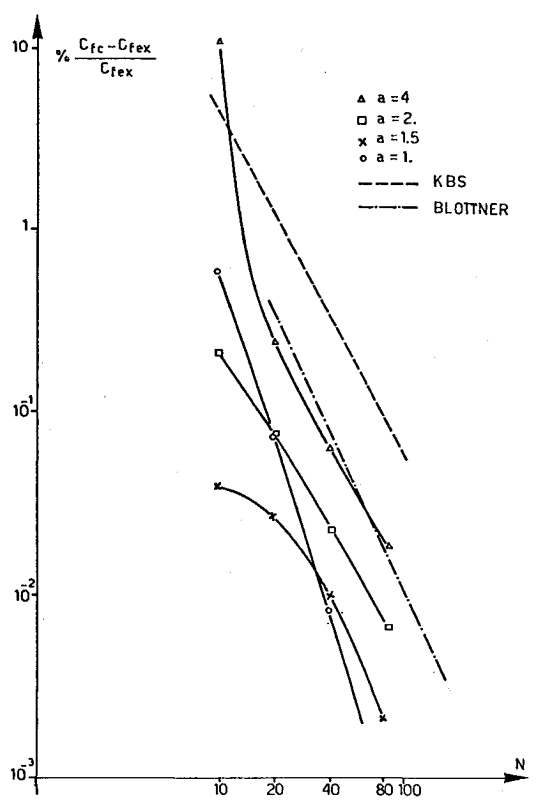

Fig. 2 Accuracy of the skin friction, with different a.

proportional to Δt. Thus the linearization of the momentum equation retains the accuracy of the time-differencing discretization. If the coordinate transformation does not depend on time $\Delta A^n = 0$, Eq. (17) assumes the form obtained by Beam and Warming, and values of $\theta = 1$ and $\theta = \frac{1}{2}$ can be used. In our case, a time-dependent transformation has been introduced; if we desire second-order accuracy with $\theta = \frac{1}{2}$ extra terms will be necessary. To avoid the need for these extra terms, second-order accuracy can be obtained with $\theta = 1$ and $\zeta = \frac{1}{2}$, which is a three-point backward discretization. However, two-level storage is required; that is, the quantities ∇p^n and Δp^n have to be stored. When applied to each term of the momentum equation in the case of $\theta = 1$, which includes the Euler implicit and the three-point backward methods, this procedure yields

$$\Delta M_l^n + M_l^n = -A^{n+1}\left[\Delta U^n\left(\frac{\partial U}{\partial x_1}\right)^n + U^n\frac{\partial \Delta U^n}{\partial x_1} + \left(U\frac{\partial U}{\partial x_1}\right)^n\right]$$

$$+B^{n+1}\left[\Delta V^n\left(\frac{\partial U}{\partial x_2}\right)^n + V^n\frac{\partial \Delta U^n}{\partial x_2} + \left(V\frac{\partial U}{\partial x_2}\right)^n\right]$$

$$+C^{n+1}\left(\frac{\partial \Delta U^n}{\partial x_2} + \frac{\partial U^n}{\partial x_2}\right) + D^{n+1}\left[\Delta U^n\left(\frac{\partial U}{\partial x_2}\right)^n\right.$$

$$\left.+U^n\frac{\partial \Delta U^n}{\partial x_2} + \left(U\frac{\partial U}{\partial x_2}\right)^n\right] + \left(\frac{\partial U_e}{\partial x} + U_e\frac{\partial U_e}{\partial t}\right)$$

$$+F^{n+1}\left[\frac{\partial}{\partial x_2}\left(E\frac{\partial U}{\partial x_2}\right)^n + \frac{\partial}{\partial x_2}\left(E\frac{\partial \Delta U^n}{\partial x_2}\right)\right] \tag{18}$$

The differentiated continuity equation (5), expressed in terms of ΔU^n and ΔV^n, will be

$$G^{n+1}\left[\frac{\partial^2 \Delta U^n}{\partial x_1 \partial x_2} + \frac{\partial^2 U^n}{\partial x_1 \partial x_2}\right] + H^{n+1}\left[\eta\frac{\partial}{\partial x_2}\left(E\frac{\partial \Delta U^n}{\partial x_2}\right)\right.$$

$$\left.+\frac{\partial \Delta U^n}{\partial x_2} + \frac{\partial}{\partial x_2}\left(E\frac{\partial U}{\partial x_2}\right)^n + \frac{\partial U^n}{\partial x_2}\right]$$

$$+L^{n+1}\left[\frac{\partial}{\partial x_2}\left(E\frac{\partial \Delta V^n}{\partial x_2}\right) + \frac{\partial}{\partial x_2}\left(E\frac{\partial V^n}{\partial x_2}\right)\right] = 0 \tag{19}$$

To solve the linear system of Eqs. (16) and (19), the finite-difference scheme of Eqs. (11) and (12) in the normal direction was used. In the downstream direction, the Euler implicit scheme was employed. With the procedure described above, the system of nonlinear partial differential equations reduces to a linear block tridiagonal system of the same form as Eq. (13). The boundary conditions [Eq. (16)] were used to evaluate the coefficients at $J = 1$ and JM, and the block tridiagonal system was solved by Gaussian elimination. Higher-order accurate schemes were not used in the streamwise direction, because the method described in this paragraph has been developed only to compare the results obtained with those of the more efficient scheme described in the next section.

C. Linearization for the Downstream Direction

It is desirable to solve the unsteady boundary-layer equations on the x-y plane at each t, especially if flow reversal occurs. The cause of this flow reversal is adverse pressure gradients, and the effect of unsteadiness is to delay and/or reduce the amount of flow reversal. Moreover, the numerical procedure can be applied to the steady boundary-layer equations. The first derivative in the downstream direction can be expressed by Eq. (15) where the n index now represents the position in the x_1 direction

$$\left[\left(\frac{\partial U}{\partial x_1}\right)^n + \theta\frac{\partial \Delta U^n}{\partial x_1}\right]\frac{\Delta x_1}{1+\zeta}$$

$$= \Delta U^n - \zeta/(1+\zeta)\,\nabla U^n + 0[(\theta - \zeta - \tfrac{1}{2})\Delta x_1^2 + \Delta x_1^3] \tag{20}$$

where the forward Δ and the backward ∇ operators relate the quantities at different positions in the streamwise direction. Multiplying Eq. (20) by U^{n+1}, we find the left-hand side becomes

$$\frac{\Delta x_1}{1+\zeta}\left[U^{n+1}\frac{\partial \Delta U^n}{\partial x_1} + \Delta U^n\left(\frac{\partial U}{\partial x_1}\right)^n + \left(U\frac{\partial U}{\partial x_1}\right)^n\right]$$

$$+(\theta - 1)\,U^{n+1}\frac{\partial \Delta U^n}{\partial x_1}\frac{\Delta x_1}{1+\zeta} \tag{21}$$

Now the difference between $U(\partial U/\partial x_1)$ at station $n+1$ and $U(\partial U/\partial x_1)$ at station n can be expressed as

$$\Delta\left(U\frac{\partial U}{\partial x_1}\right)^n = U^{n+1}\frac{\partial \Delta U^n}{\partial x_1} + \Delta U^n\left(\frac{\partial U}{\partial x_1}\right)^n + 0(\Delta U^2) \tag{22}$$

Thus, Eq. (21) will contain only $\Delta[U(\partial U/\partial x_1)]^n$ and $[U(\partial U/\partial x_1)]^n$ provided $\theta = 1$, i.e., only for the Euler implicit and three-point backward schemes. Then Eq. (21) can be written

$$\frac{\Delta x_1}{1+\zeta}\left[\Delta\left(\frac{M_{x_1}}{A}\right)^n + \left(\frac{M_{x_1}}{A}\right)^n\right] \tag{23}$$

where M_{x_1} is defined by writing the momentum equation as $AU(\partial U/\partial x_1) = M_{x_1}$. For $\theta \neq 1$, the last term in Eq. (21) cannot be expressed in terms of M_{x_1}. This prevents us from using the Crank/Nicolson scheme ($\theta = \frac{1}{2}$, $\zeta = 0$) in the downstream direction. In the case of $\theta = 1$, Eq. (20) multiplied by U^{n+1} becomes

$$\frac{[\Delta(M_{x_1}/A)^n + (M_{x_1}/A)^n]}{1+\zeta}\Delta x_1$$

$$= U^n\Delta U^n - \zeta/(1+\zeta)\,U^n\nabla U^n + 0(\Delta U^n)^2$$

$$+0[(\tfrac{1}{2} - \zeta)\Delta x_1^2 + \Delta x_1^3] \tag{24}$$

It can be seen that, with the three-point backward scheme ($\zeta = \frac{1}{2}$), the first-order truncation error due to the discretization of $(\partial U/\partial x_1)$ is eliminated, and the accuracy of Eq. (24) is of the order of $(\Delta U^n)^2$. Adopting the procedure used to derive Eq. (17), the left-hand side of Eq. (24) becomes

$$\Delta\left(\frac{M_{x_1}}{A}\right)^n + \left(\frac{M_{x_1}}{A}\right)^n = -\frac{1}{A^{n+1}}\left\{\left[\frac{\partial \Delta U^n}{\partial t} + \left(\frac{\partial U}{\partial t}\right)^n\right]\right.$$

$$+B^{n+1}\left[\Delta V^n\left(\frac{\partial U}{\partial x_2}\right)^n + V^n\frac{\partial \Delta U^n}{\partial x_2} + V^n\left(\frac{\partial U}{\partial x_2}\right)^n\right]$$

$$+C^{n+1}\left(\frac{\partial \Delta U^n}{\partial x_2} + \frac{\partial U^n}{\partial x_2}\right) + D^{n+1}\left[\Delta U^n\left(\frac{\partial U}{\partial x_2}\right)^n\right.$$

$$\left.\left.+U^n\frac{\partial \Delta U^n}{\partial x_2} + \left(U\frac{\partial U}{\partial x_2}\right)^n\right]\right\} + \frac{1}{A^{n+1}}\left(\frac{\partial U_e}{\partial t} + U_e\frac{\partial U_e}{\partial x}\right)^{n+1}$$

$$+\frac{F^{n+1}}{A^{n+1}}\left[\frac{\partial}{\partial x_2}\left(E\frac{\partial U}{\partial x_2}\right)^n + \frac{\partial}{\partial x_2}\left(E\frac{\partial \Delta U^n}{\partial x_2}\right)\right] \tag{25}$$

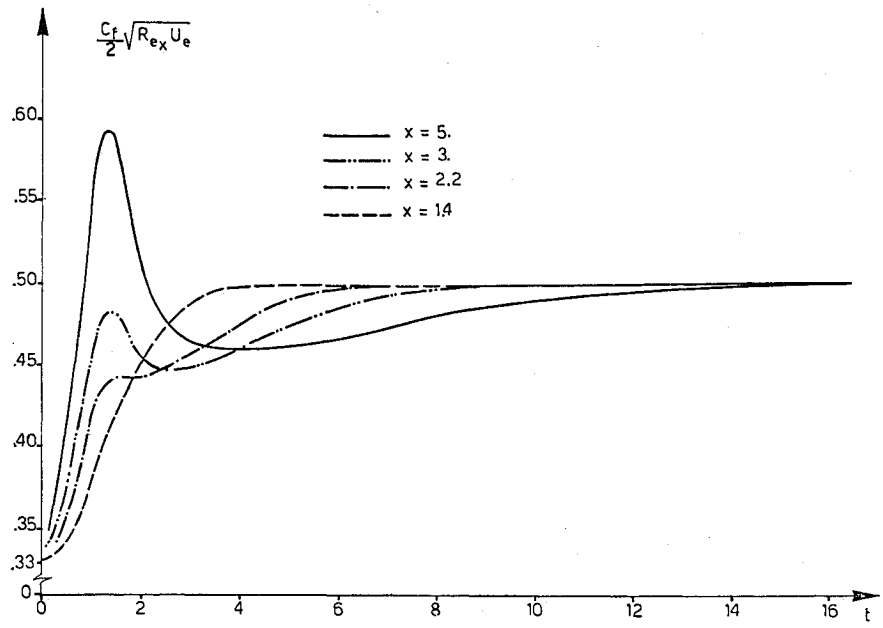

Fig. 3 Skin friction for the transition to Falkner-Skan flow case.

The linearization procedure applied to differencing the momentum equation in the downstream direction must be applied also to the differentiated continuity equation (5). The general formulation will be

$$\left[\Delta\left(\frac{C_{x_1}}{G}\right)^n+\left(\frac{C_{x_1}}{G}\right)^n\right]\frac{\Delta x_1}{1+\zeta}$$

$$=\frac{\partial}{\partial x_2}\Delta U^n-\frac{\zeta}{1+\zeta}\frac{\partial \nabla U^n}{\partial x_2}+0[(\tfrac{1}{2}-\zeta)\Delta x_1^2+\Delta x_1^3] \quad (26)$$

where C_{x_1} is defined by writing Eq. (5) as $G\partial^2 U/\partial x_1\partial x_2=C_{x_1}$. Using the same procedure employed for the momentum equation, the left-hand side of Eq. (26) becomes

$$\Delta\left(\frac{C_{x_1}}{G}\right)^n+\left(\frac{C_{x_1}}{G}\right)^n=-\frac{H^{n+1}}{G^{n+1}}\left[\eta\frac{\partial}{\partial x_2}\left(E\frac{\partial\Delta U^n}{\partial x_2}\right)+\frac{\partial\Delta U^n}{\partial x_2}\right.$$

$$\left.+\eta\frac{\partial}{\partial x_2}\left(E\frac{\partial U}{\partial x_2}\right)^n+\left(\frac{\partial U}{\partial x_2}\right)^n\right]$$

$$-\frac{L^{n+1}}{G^{n+1}}\left[\frac{\partial}{\partial x_2}\left(E\frac{\partial\Delta V^n}{\partial x_2}\right)+\frac{\partial}{\partial x_2}\left(E\frac{\partial V}{\partial x_2}\right)^n\right] \quad (27)$$

Discretizing the system of Eqs. (24) and (26) in the normal direction using the finite-difference scheme given by Eqs. (11) and (12) and using an Euler implicit scheme to discretize the time derivative, a block tridiagonal system of the same form as Eq. (13) is found.

IV. Results

To test the method, several laminar flows for which experimental and analytical solutions were available have been considered.

A. Transition to Falkner-Skan Flow

The first case is a boundary layer generated by a pressure gradient that, in time, starts from zero (Blasius flow) and goes to a distribution which has a self-similar solution (Falkner-Skan flow). This pressure gradient gives the edge velocity

$$U_e=1-f(t)\,(x^m-1) \qquad (x\geq 1) \quad (28)$$

$$f(t)=(10-15t^*+6t^{*2})t^{*3} \qquad (0\leq t^*\leq 1) \quad (29)$$

where $t^*=t/2$.

The function $f(t)$ gives a smooth transition from $t=0$ to $t=2$; for t greater than 2, the pressure gradient is frozen at the Falkner-Skan one. The initial condition at $t=0$ and $x\geq 1$ is steady Blasius flow found by solving the system of Eq. (8) with $m=0$. At $x=1$ and $t\geq 0$, a quasisteady flow has been assumed, given by the solution of the system of Eqs. (8) with m replaced by $m\cdot f(t)$.

To solve for this flow, both methods described in Secs. IIIB and IIIC were employed and gave the same results when the same order of accuracy was employed. Figure 3 shows the evolution in time of the skin friction at different x stations for $m=+0.1$. As expected the flow becomes self-similar at later times, with increasing downstream distance. The sharp increase of the skin friction in the transition region is due to the unsteady part of the pressure gradients. The calculated nondimensional skin friction at $t\gg 0$ is in good agreement with the value for the steady Falkner-Skan flow at $m=0.1$ ($C_f/2\sqrt{Re_x}U_e=0.4966$).

B. Oscillatory Blasius Flow

This flow has been investigated both analytically and experimentally since 1954.[10] The edge velocity can be expressed as

$$U_e=1+U_1\sin\omega t \quad (30)$$

The initial conditions for both the $x=x_0$ and the $t=0$ planes were assumed to be Blasius flow. The transformation of Eq. (3) does not allow treatment of the singularity at the stagnation point; thus x_0 was chosen to be somewhat downstream of the stagnation point. The boundary-layer thickness was assumed to grow as $\delta\simeq\sqrt{x/Re}$ in order to allow comparison with the results available in the literature. The horizontal velocity profile can be represented by $U=U_0(x)+\delta U_1(x,y)\sin[\omega t+\gamma(x,y)]$, and the amplitude of the velocity oscillations and their phase angles relative to the mainstream oscillations were calculated using the procedure of Cebeci.[11] In Figs. 4 and 5, we plot the profile of the amplitude of the velocity oscillations vs η at low frequency. For comparison we have also plotted the analytical results of Lighthill[10] and the experimental ones of Hill.[12] The agreement with experimental results is better at larger values of the frequency parameter $x\omega$. This is not surprising, as the Lighthill theory is valid at very low $x\omega$. In Figs. 7 and 8 we plot the phase angle of the velocity oscillations vs η at two frequencies. Again, the agreement with the experimental and analytical results is good. The computation for this case was

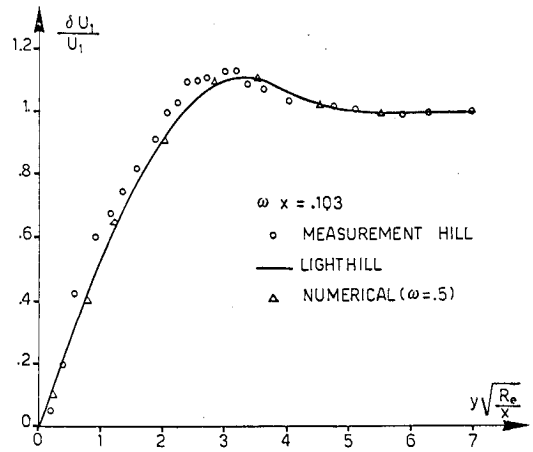

Fig. 4 Amplitude of low-frequency velocity oscillations.

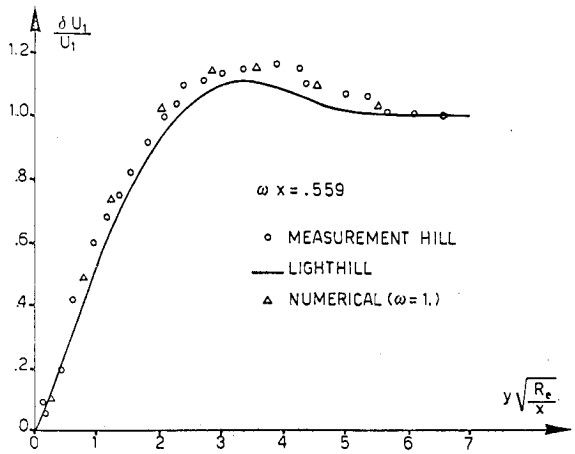

Fig. 5 Amplitude of intermediate-frequency velocity oscillations.

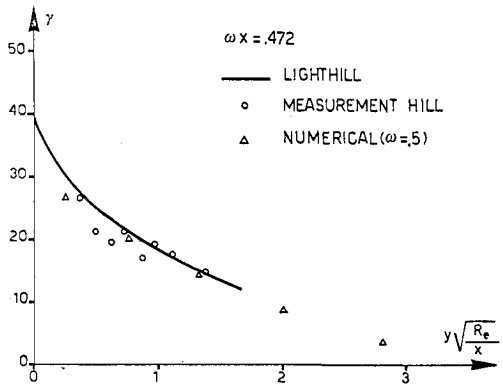

Fig. 6 Phase of low-frequency velocity oscillations.

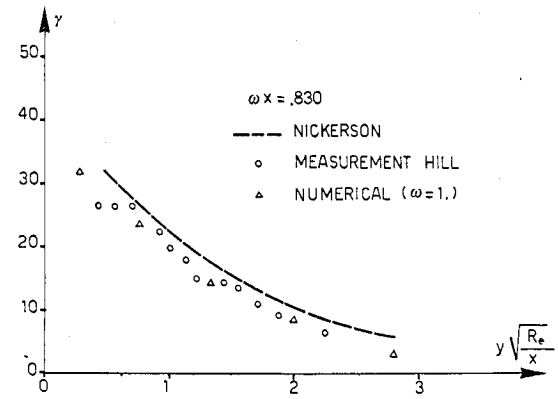

Fig. 7 Phase of intermediate-frequency velocity oscillations.

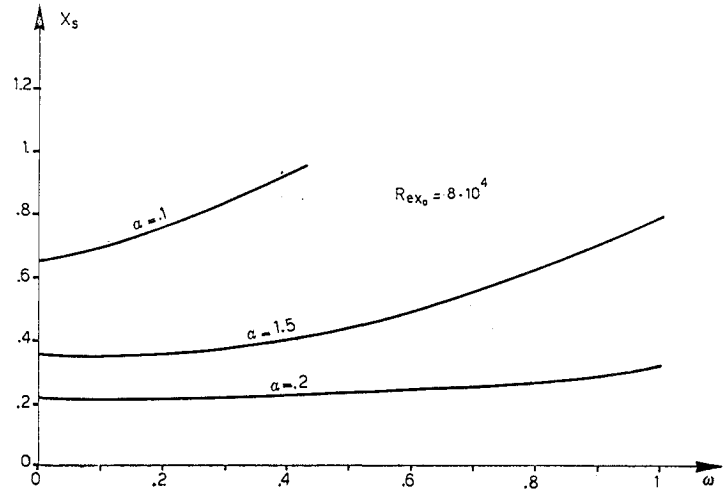

Fig. 8 Separation behavior at $Re_{x_0} = 8 \cdot 10^4$.

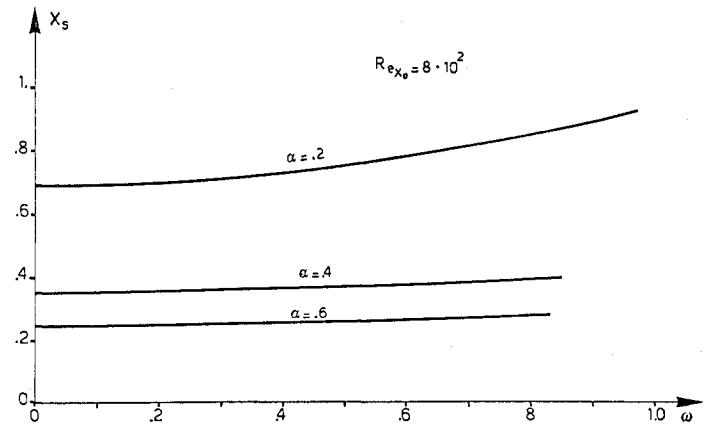

Fig. 9 Separation behavior at $Re_{x_0} = 8 \cdot 10^2$.

done using the method described in Sec. IIIC. Starting at $t=0$, we computed for six cycles of the edge velocity, but three cycles would have been sufficient.

C. Oscillatory Howarth Flow

This flow is of particular interest as it introduces a region of separated flow, which has application to helicopter rotor blades, especially at intermediate values of the characteristic frequency ωx. The edge-velocity profile is given by

$$U_e = 1 - \tfrac{1}{2}\alpha(x - x_0)(1 - \cos\omega t) \qquad (31)$$

To overcome the discontinuity of the derivative at $x = x_0$, smoothing was done is such a way as to have

$$(\partial U_e/\partial x)(x_{0,t}) = 0$$

A Blasius flow is assumed at $x \leq x_0$. If only the steady part of Eq. (31) is considered, the Twaites method[9] can be used to calculate the separation point, which depends on both x_0 and α. The effect of the unsteadiness is to move the separation point farther downstream as the frequency ω is increased. In Figs. 8 and 9, a map of the point of zero skin friction vs the parameter ω at different values of α is given for two values of Re_{x_0}.

The effect of unsteadiness is higher at small values of α, as shown in Fig. 9. At larger values of α, the delay of separation is very small. The positions of the separation point for $\omega=0$ were calculated and are in good agreement with the values calculated by the Twaites method.

All of the cases considered above used 41 mesh points in the normal direction. A bigger mesh size could be used, as can be seen from Fig. 2. In the downstream direction, both uniform and stretched coordinates were used and no difference was found. The time step used in the oscillatory flows was $\Delta t=2\pi/(40\ \omega)$. The computer time needed to solve case B for six cycles with this grid was 20 s on a CDC 7600.

V. Conclusions

A fully implicit, noniterative method has been developed to solve the unsteady and steady boundary-layer equations accurately and very efficiently. This method has been developed particularly for the purpose of treating the turbulent boundary layer, as has been shown by results published elsewhere.[13,14] The main features of the method are: it does not employ similarity coordinate transformations that are valid only for laminar boundary layer, and the implicit noniterative scheme allows a fast coupling between the mean velocity field and the mean turbulent quantities. We think that the second characteristic is a great improvement compared to previous numerical methods that usually treat the turbulent quantities explicitly. The only disadvantage of this method is that it is first-order accurate in the streamwise direction.

More work is needed if we are to treat small separation bubbles in which the boundary-layer approximations are valid. In this case, to allow use of a noniterative procedure, the convective terms must be approximated in the reverse flow region by the Flügge-Lotz and Reyhner approximation $U\partial U/\partial x=0$ for $U<0$, which has been shown to give results as good as those obtained by upwind differencing in the laminar case.[15] If upwind differencing were used, extrapolation could be used to find the velocities downstream in the separated flow region. This approach has been used to solve this problem for laminar frozen flows, and they have been compared with the results obtained solving the full Navier-Stokes equations[16] without finding good agreement. The cause is the sensitivity of the separation to small changes of the external velocity distribution in the laminar case.

Acknowledgments

The authors express gratitude to the Ames Research Center for the support of this work through the use of the CDC 7600 at the Center. Gratitude is also expressed to Prof. W.C. Reynolds for useful discussions. Through a junior fellowship, NATO supported Dr. Orlandi at Stanford in 1978.

References

[1] Blottner, F.G., "Investigation of Some Finite-Difference Techniques for Solving the Boundary Layer Equations," *Computer Methods in Applied Mechanics and Engineering,* Vol. 6, July 1975, pp. 1-30.

[2] Keller, H.B., "Numerical Methods in Boundary Layer Theory," *Annual Review of Fluid Mechanics,* Vol. 10, 1978, pp. 417-433.

[3] Singleton, R.E. and Nash, J.F., "Method for Calculating Unsteady Turbulent Boundary Layers in Two and Three-Dimensional Flows," *AIAA Journal,* Vol. 12, May 1974, pp. 590-595.

[4] Briley, W.R. and McDonald, H., "Solution of Three-Dimensional Compressible Navier-Stokes Equations by an Implicit Technique," *Proceedings of the Fourth International Conference on Numerical Methods in Fluid Dynamics,* Boulder, Colo., June 1974, Springer-Verlag, New York/Berlin, 1975.

[5] Warming, R.F. and Beam, R.M., "On the Construction and Application of Implicit Factored Schemes for Conservative Laws," *Symposium on Computational Fluid Dynamics, SIAM-AMS Proceedings,* Vol. 11, 1977.

[6] Beam, R.M. and Warming, R.F., "An Implicit Factored Scheme for the Compressible Navier-Stokes Equations," *AIAA Journal,* Vol. 16, April 1978, pp. 393-402.

[7] Cunsolo, D. and Orlandi, P., "Accuracy in Non-Orthogonal Grid Reference Systems," *Proceedings of Numerical Methods in Laminar and Turbulent Flow,* Swansea, July 1978.

[8] Blottner, F.G., "Variable Grid Scheme Applied to Turbulent Boundary Layers," *Computer Methods in Applied Mechanics and Engineering,* Vol. 4, July 1974, pp. 174-194.

[9] Cebeci, T. and Bradshaw, P., "Momentum Transfer in Boundary Layers," *Series in Thermal and Fluids Engineering,* McGraw-Hill Book Co., Hemisphere Publishing Corp., Washington/London, 1977.

[10] Lighthill, M.J., "The Response of Laminar Skin Friction and Heat Transfer to Fluctuations in the Stream Velocity," *Proceedings of the Royal Society of London*, Ser. A, Vol. 224, June 1954, pp. 1-23.

[11] Cebeci, T., "Calculations of Unsteady Two-Dimensional Laminar and Turbulent Boundary Layers with Fluctuations in External Velocity," *Proceedings of the Royal Society of London,* Ser. A, Vol. 355, June 1977, pp. 225-238.

[12] Hill, P.G. and Stenning, A.H., "Laminar Boundary Layers in Oscillatory Flow," *Transactions of the ASME, Journal of Basic Engineering,* Vol. 82, Sept. 1960, pp. 593-607.

[13] Orlandi, P. and Reynolds, W.C., "A Provisional Model for Unsteady Turbulent Boundary Layers," submitted to *AIAA Journal.*

[14] Orlandi, P., "Implicit Non-Iterative Schemes for Turbulent Unsteady Boundary Layers," *7th International Conference on Numerical Methods in Fluid Dynamics,* Stanford, Calif., June 1980, Springer-Verlag, New York and Berlin, 1981.

[15] Carter, J.E., "Solutions for Laminar Boundary Layers with Separation and Reattachment," AIAA Paper 74-583, 1974.

[16] Briley, W.R., "A Numerical Study of Laminar Separation Bubbles Using the Navier-Stokes Equations," *Journal of Fluid Mechanics,* Vol. 47, Pt. 4, June 1971, pp. 713-736.